IDENTIFICATION OF MOTIVES MEDIATING ALTERNATIVE FUNCTIONS OF THE NEOMORPHIC MOONLIGHTING TPPP/p25

Natália Tőkési[a*], Judit Oláh[a*], Emma Hlavanda[a], Sándor Szunyogh[a], Adél Szabó[a], Fruzsina Babos[b], Anna Magyar[b], Attila Lehotzky[a], Elemér Vass[c], Judit Ovádi[a§]

[a]Institute of Enzymology, Research Centre for Natural Sciences, Hungarian Academy of Sciences, 1113 Budapest, Hungary

[b]Research Group of Peptide Chemistry, Hungarian Academy of Sciences, Eötvös Loránd University, 1117 Budapest, Hungary

[c]Department of Organic Chemistry, Institute of Chemistry, Eötvös Loránd University, 1117 Budapest, Hungary

*These authors contributed equally to this work.

[§] Address correspondence to: Judit Ovádi, Institute of Enzymology, Research Centre for Natural Sciences, Hungarian Academy of Sciences, Budapest, Karolina út 29., H-1113, Hungary, Tel. (36-1) 279-3129; Fax. (36-1) 466-5465; E-mail: ovadi.judit@ttk.mta.hu

E-mail addresses:

NT: tokesi.natalia@ttk.mta.hu; J. Oláh: olah.judit@ttk.mta.hu;

EH: hlavanda.emma@gmail.com; SSZ: szunyogh@enzim.hu;

ASZ: szaboadel90@gmail.com; FB: babosfruzsi@gmail.com;

AM: magyar@chem.elte.hu; AL: lehotzky.attila@ttk.mta.hu;

EV: evass@chem.elte.hu; J. Ovádi: ovadi.judit@ttk.mta.hu

ABSTRACT

The disordered Tubulin Polymerization Promoting Protein (TPPP/p25), a prototype of neomorphic moonlighting proteins, displays physiological and pathological functions by interacting with distinct partners. Here the role of the disordered N- and C- termini straddling a middle flexible segment in the distinct functions of TPPP/p25 was established, and the binding motives responsible for its heteroassociations with tubulin and α-synuclein, its physiological and pathological interacting partner, respectively, were identified. We showed that the truncation of the disordered termini altered the folding state of the middle segment and has functional consequences concerning its physiological function. Double truncation diminished its binding to tubulin/microtubules, consequently the tubulin polymerization/microtubule bundling activities of TPPP/p25 were lost highlighting the role of the disordered termini in its physiological function. In contrast, interaction of TPPP/p25 with α-synuclein was not affected by the truncations and its α-synuclein aggregation promoting activity was preserved, showing that the α-synuclein binding motif is localized within the middle segment. The distinct tubulin and α-synuclein binding motives of TPPP/p25 were also demonstrated at the cellular level: the double truncated TPPP/p25 did not align along the microtubules in contrast to the full length form, while it induced α-synuclein aggregation. The localization of the binding motives on TPPP/p25 were established by specific ELISA experiments performed with designed and synthesized peptides: motives at the 178-187 and 147-156 segments are involved in the binding of tubulin and α-synuclein, respectively. The dissimilarity of these binding motives responsible for the neomorphic moonlighting feature of TPPP/p25 has significant innovative impact in anti-Parkinson drug research.

KEYWORDS

α-synuclein, binding motives, neomorphic moonlighting function, TPPP/p25

1. INTRODUCTION

The recognition that there are proteins with more than one function was recognized two decades ago and this characteristic was termed first as gene sharing and later as moonlighting [1-3]. Moonlighting proteins perform multiple, independent functions that are not coded at gene level, do not stem from genetic alterations (gene fusion, splice variants or mutations), these functions are manifested at the protein level. The functions of these moonlighting proteins can vary as a consequence of changes in cellular localization, cell type, oligomeric state, concentrations of substrates, cofactors or products [3]. Moonlighting should also be distinguished from multifunctionality of proteins, in which a protein has multiple domains, each fulfilling a different function [2]. Recently a subclass of the moonlighting proteins has been defined as Neomorphic Moonlighting Proteins in which conformational changes and/or interactions with distinct partners other than at normal conditions impart a pathological function [4]. Therefore, in the case of these moonlighting proteins the physiological function could be converted into a pathological one [4-5].

Moonlighting is characteristic for many disordered proteins which do not have stable, well-defined 3D structures thus can adapt conformations upon binding to their partners [6-7]. Proteins with such features are rather common in living cells. They perform essential functions such as regulation of transcription and translation or cellular signal transduction [6, 8]. Besides that, disordered proteins also play crucial roles in the etiology of conformational diseases such as Parkinson's (PD) and Alzheimer's diseases [9-10].

Tubulin Polymerization Promoting Protein (TPPP/p25) is an intrinsically disordered protein, its extended unstructured N- and C-terminal regions (45 and 44 aa) are straddling a middle flexible segment (130 aa) [11]. It is considered as a prototype of the neomorphic moonlighting proteins as under physiological and pathological conditions it performs multiple functions depending on its interacting partners. TPPP/p25 was isolated and identified as a brain-specific protein [12] and on the basis of its in vitro function and apparent molecular mass it was denoted TPPP/p25 [13]. Physiologically TPPP/p25 is expressed mainly in the oligodendrocytes [14] of brain and plays a crucial role in their differentiation process [15]. Its major physiological interacting partner is the tubulin/microtubule network and it modulates microtubule dynamics and organization via its microtubule bundling activity enhancing microtubule stability [13, 16-17]. In fact, TPPP/p25 also interacts with the tubulin deacetylase enzyme, HDAC6, and inhibits its deacetylase activity and thus plays a role in the control of the acetylation level of microtubules [17]. In addition, TPPP/p25 binds GTP and catalyzes its hydrolysis in a Mg^{2+}-dependent manner in vitro [11].

The non-physiological expression level of TPPP/p25 is coupled with distinct central nervous system diseases such as multiple sclerosis (altered expression in the brain and increased TPPP/p25 level in the cerebrospinal fluid of the patients) [18-19], oligodendrogliomas (lack of TPPP/p25 expression) [20] or conformational diseases (co-enrichment of TPPP/p25 and α-synuclein in inclusion bodies) [21]. The development of the conformational diseases originates from the formation of aberrant protein-protein interactions leading to protein aggregation and pathological inclusion body formation. It has recently been reported that TPPP/p25 interacts with α-synuclein and β-amyloid and promotes their aggregation in vitro [22-23]. The

involvement of TPPP/p25 in such pathological associations leads to the etiology of PD and Multiple System Atrophy as we demonstrated earlier [21].

In this paper the structural and functional roles of the disordered termini of TPPP/p25 were characterized in its physiological and pathological functions, in addition, the tubulin and the α-synuclein binding motives of TPPP/p25 involved within these functions were identified.

2. MATERIALS AND METHODS

2.1 Synthesis of the peptides

The peptides BF180-183 were synthesized manually by Solid Phase Peptide Synthesis (SPPS), using Fmoc/tBu chemistry on 4-methylbenzhydrylamine resin. The biotinylated forms were made using biotinyl-6-amino-hexanoic acid (long chain biotin). In the case of BF183 and BF180 a Lys was built into the C-terminus of the peptides to conjugate the biotin derivative to its side chain (ε-amino group). The N-terminus of the peptides was acetylated, while the C-terminus was in amide form. The peptides were cleaved from the resin with anhydrous HF in the presence of p-cresol at 0 °C. The P1-P4 peptides were synthesized by automated SPPS (Syro2000; MultiSynTech GmbH, Germany), using Fmoc/tBu strategy on 4-methylbenzhydrylamine resin with double-coupling protocol. A Cys was built into the N-terminus of the peptides. The N-terminus of the peptides was acetylated, while the C-terminus was in amide form. The peptides were cleaved from the resin with trifluoroacetic acid in the presence of scavengers (ethanedithiol, tioanizol, H_2O, phenol). The crude products in each case were purified by reversed-phase chromatography and the purified compounds were characterized by analytical RP-HPLC and mass spectrometry (PE-SCIEX API-2000 triple quadrupole instrument, Perkin-Elmer).

2.2 DNA manipulations

Prokaryotic expression vectors containing inserts for human full length TPPP/p25 and N-terminal truncated TPPP/p25 by amino acid residues 3–43 (TPPP/p25 delta 3-43) were prepared and purified as described previously [17]. C-terminal truncated TPPP/p25 by residues 175-219 (TPPP/p25 delta 175-219) was amplified by polymerase chain reaction (PCR) using forward primer 5'- AGATACACATATG GCTGACAAGGCTAAGC-3', and reverse primer 5'- GGTGCTCGAGGCCCG TGAACTTGGTGGTGTC-3'. The double truncated TPPP/p25 corresponding to amino acid residues 44–174 (TPPP/p25 delta 3-43/delta 175-219) was amplified by PCR using forward primer 5'- GAGATATACATATGGCTGCATCCCCTGAGCTC-3' and reverse primer 5'- GGTGCTCGAGGCCCGTGAACTTGGTGGTGTC -3'. After digestion with NdeI and XhoI restriction enzymes inserts were ligated into pET21c vector (Novagen). Eukaryotic expression vectors containing inserts for human full length TPPP/25 (pEGFP-TPPP/p25) were prepared as described previously [16]. The double truncated TPPP/p25 (pEGFP-TPPP/p25 delta 3-43/delta 175-219) was amplified by PCR using the following primer pairs: 5'-GGAATTC TATGGCTGCATCCCCTGAG-3'; 5'-ATGGATCCCTAGCCCGTGAACTTGGT-3' and pEGFP-TPPP/p25 as a template. After digestion with EcoRI and BamHI restriction enzymes inserts were ligated into pEGFP-C1 vector (Clontech). Correct insertion of all these plasmids was verified by DNA sequencing.

2.3 Recombinant TPPP/p25 protein purification

Human recombinant TPPP/p25 forms possessing a His-tag were expressed in E. coli BL21 (DE3) cells and isolated on HIS-Select™ Cartridge (Sigma-Aldrich) as described previously [19, 21]. Protein concentrations were determined from the absorbance at 280 nm using an extinction coefficient of 10095 M^{-1} *cm^{-1}, 10095 M^{-1}

*cm^{-1}, 5625 M^{-1} *cm^{-1} and 5625 M^{-1} *cm^{-1} for TPPP/p25, N-terminal truncated TPPP/p25, C-terminal truncated TPPP/p25 and double truncated TPPP/p25, respectively.

2.4 Tubulin preparation

Tubulin was prepared from bovine brain according to the method of Na and Timasheff [24].

2.5 α-synuclein purification

Human recombinant α-synuclein was prepared as described previously [25]. Protein concentration was determined from the absorbance at 280 nm using an extinction coefficient of 5960 M^{-1} *cm^{-1}.

2.6 Circular dichroism (CD) spectroscopy

CD measurements were performed on Jasco J-720 spectropolarimeter at 20 nm/min scan rate, 8 s time constant and 0.5 nm step size in 10 mM phosphate buffer, pH 7.2 at room temperature. The path length was 0.1 cm. The protein concentrations were 4 μM for TPPP/p25 forms and 1 μM for tubulin. The reaction mixtures were incubated for 10 minutes before recording the spectra. Scanning was repeated three times, and the spectra were averaged. Mean molar ellipticity per residue (Θ) in degrees square centimeter per decimole was calculated according to the following equation: $\Theta = \Theta_m/(10*n*c*l)$, where Θ_m is the measured ellipticity in millidegrees, n is the number of amino acid residues, c is the concentration in moles and l is the path length of the cell in centimetres.

2.7 Fourier transformed infrared spectroscopy (FT-IR)

FT-IR spectra of the different TPPP/p25 forms were recorded with a Bruker Equinox55 FT-IR spectrometer equipped with a liquid-nitrogen-cooled MCT detector. The proteins (1 mM) were dissolved in 12 mM phosphate buffer containing 110 mM

NaCl with D_2O at pD 6.0. Spectra were obtained by co-adding 128 scans at a spectral resolution of 4 cm^{-1} in a BaF_2 cell with a 50 μm spacer.

2.8 Limited proteolysis

TPPP/p25 forms at 1 mg/ml were digested with 0.01 mg/ml chymotrypsin (Sigma-Aldrich) in 50 mM tris(hydroxymethyl)aminomethane buffer pH 8.0 containing 10 mM $CaCl_2$ at room temperature. A control sample did not contain protease. Aliquots were drawn from each sample at different time points. The digestion was terminated by 1 mM 4-(2-aminoethyl) benzenesulfonyl fluoride hydrochloride. The samples were analyzed by sodium dodecyl sulfate polyacrylamide gel electrophoresis (SDS-PAGE), separated on a Tricin-containing two-layer-gel and stained with Coomassie Brilliant Blue R-250 containing 2-mercaptoethanol and dithioerythritol (DTE).

2.9 Fluorescence spectroscopy

Thioflavin T fluorescence. TPPP/p25 proteins (10 μM) without and with α-synuclein (150 μM) were incubated for 3-4 days at 37 °C in phosphate buffered saline (PBS) buffer. Then a 10 μl aliquot was added to 1 ml 10 μM thioflavin T solution in 100 mM glycine buffer, pH 8.55. The fluorescence spectra were measured on a FluoroMax-3 spectrofluorometer (Jobin Yvon Inc.), using thermostated quartz cuvettes of 1 cm optical path length at 37 °C. Data were processed using DataMax software. Scanning was repeated three times, and the spectra were averaged, the buffer spectrum was subtracted in each case. Spectra were recorded at an excitation wavelength (λ_{ex}) of 440 nm (slit width 4 nm), emission spectra were collected from 450 to 600 nm (slit width 4 nm).

1-anilino naphthalene-8-sulfonic acid (ANS) fluorescence. Fluorescence spectroscopy measurements were performed in 10 mM phosphate buffer, pH 7.2 using a Fluoromax-3 spectrofluorometer (Jobin Yvon Inc.) in a quartz cuvette of 1 cm optical

path length at 25 °C. Excitation wavelength was 380 nm, while the emission was monitored from 400 to 600 nm with 2 nm slits. The data of at least three parallel measurements were evaluated using DataMax software. 10 mM ANS (Sigma-Aldrich) stock solution was freshly prepared in distilled water. Concentrations of TPPP/p25 forms and ANS were 2.5 and 50 μM, respectively.

2.10 Enzyme-linked immunosorbent assay (ELISA)

The plate was coated with 5 μg/ml (100 μl/well) TPPP/p25 forms in PBS overnight at 4 °C. The wells were blocked with 1 mg/ml bovine serum albumin (BSA) in PBS for 1 h at room temperature. Next, the plate was incubated with serial dilutions of α-synuclein for 1 h at room temperature in PBS. In the case of the competitive ELISA, the plate was incubated with 500 nM α-synuclein preincubated without or with the biotinylated peptides (10 and 20 μM). Then the plate was sequentially incubated with α-synuclein antibody (1:5000, Sigma-Aldrich) and with the peroxidase conjugated secondary IgG (1:5000, Sigma-Aldrich). Both antibodies were in PBS buffer containing 1 mg/ml BSA, and incubated for 1 h at room temperature. Between each incubation step the wells were washed thrice with PBS containing 0.05% Tween 20 for 10 min. The presence of antibodies was detected using o-phenylenediamine in the concentration of 3.7 mM with 0.03% H_2O_2 as substrate solution. The reaction was stopped after 10 min with 1 M H_2SO_4, and the absorbance was read at 490 nm with a Wallace Victor 2 multiplate reader (Perkin Elmer). In the case of the biotinylated peptides, the plate was coated with 5 μg/ml (100 μl/well) streptavidin solution in PBS overnight at 4 °C, and the wells were blocked with 1 mg/ml BSA in PBS for 1 h at room temperature. Then the plate was incubated with 25 μg/ml solution of the biotinylated peptides for 1 h at room temperature in PBS. Next, the plate was

incubated with serial dilutions of α-synuclein, and the interaction was detected as described above.

In the case of P1-P4 peptides, Sulfhydryl-BIND™ (Maleimide) Modified Surface plate (Corning Incorporated) was used according to the manufacturer's instructions. Briefly, the plate was coated with 5 μg/ml (100 μl/well) peptide or TPPP/p25 solution in fresh PBS buffer containing 1 mM ethylenediamine tetraacetic acid pH 6.5 for 1 h at room temperature. The wells were blocked with 0.2% non-fat dry milk in PBS for 30 min at room temperature. Next, the plate was incubated with serial dilutions of tubulin for 30 min at room temperature in PBS. Then the plate was sequentially incubated with tubulin antibody (1:5000, Sigma-Aldrich), and with the corresponding peroxidase conjugated secondary IgG (1:5000, Sigma-Aldrich). o-phenylenediamine was used as substrate solution as described above.

2.11 Turbidity measurements

The assembly of tubulin (7 μM) was assessed in polymerization buffer (50 mM 2-(N-morpholino)ethanesulfonic acid buffer pH 6.6 containing 100 mM KCl, 1 mM DTE, 1 mM $MgCl_2$ and 1 mM ethylene glycol tetraacetic acid) at 37 °C. The tubulin polymerization into microtubules was induced by the addition of 3 μM of the different TPPP/p25 forms. In another set of experiments, the polymerization of 10 μM tubulin into microtubules was induced by the addition of 20 μM paclitaxel then subsequently 3 μM TPPP/p25 proteins were added to the solution. The optical density was monitored at 350 nm by a Cary 100 spectrophotometer (Varian).

2.12 Pelleting experiment

Tubulin (5 μM) was incubated with the different TPPP/p25 forms (10 μM) for 10 min at 37 °C in polymerization buffer (50 mM 2-(N-morpholino)ethanesulfonic acid buffer pH 6.6 containing 100 mM KCl, 1 mM DTE, 1 mM $MgCl_2$ and 1 mM ethylene

glycol tetraacetic acid). After centrifugation at 17000 g for 15 min at 37 °C, the pellet and the supernatant fractions were separated. The pellet fraction was washed and resuspended in buffer. Then the pellet and the supernatant fractions were analyzed by SDS-PAGE, separated on a Tricine-containing two-layer-gel and stained with Coomassie Brilliant Blue R-250 containing 2-mercaptoethanol and DTE.

2.13 Cell Culture and Manipulation

HeLa and CHO10 cells were grown and transfected as described previously [16-17]. For microscopic analysis cells were grown on 12 mm diameter coverslips and on 24-well plates for immunoblotting. 5 μM MG132 (Sigma-Aldrich) was added for 4 hours, where indicated. Uptake of TPPP/p25 forms and/or α-synuclein was investigated by the addition of 2.5/10 μg recombinant proteins into the medium freshly dissolved in PBS buffer with or without a short preincubation.

2.14 Immunocytochemistry

HeLa and CHO10 cells were fixed with ice-cold methanol for 10 minutes. After washes with PBS, samples were blocked for 30 minutes in PBS-0.1% Triton X-100 containing 5% fetal calf serum. Subsequently, the cells were stained with a monoclonal antibody against α-tubulin (Sigma-Aldrich), a monoclonal antibody against α-synuclein (Sigma-Aldrich) and polyclonal rat sera against human recombinant TPPP/p25 [21] followed by Alexa 488 conjugated anti-mouse antibody and Alexa 546 conjugated anti-rat antibody (Invitrogen). The samples were washed thrice with PBS after antibody incubation. Nuclei were counterstained with 4,6-diamidino-2-phenylindole (DAPI). For samples containing α-synuclein, Triton–X-100 was changed to 30 μM digitonin, otherwise the protocol remained the same. Images of fixed samples were acquired on a Leica DMLS microscope. Figure 4 was imaged on Zeiss LSM710 confocal microscope.

2.15 Immunoblotting

The uptake of TPPP/p25 by HeLa/CHO10 cells was detected by immunoblotting as described previously [17] using a polyclonal rat serum against human recombinant TPPP/p25 [21]. The loading control was glyceraldehyde 3-phosphate dehydrogenase (GAPDH) detected by a monoclonal GAPDH antibody (Calbiochem).

3. RESULTS AND DISCUSSION

3.1 Structural characterization of the TPPP/p25 forms

Previously we reported that TPPP/p25 is an intrinsically disordered protein with extended unstructured N- and C-terminal regions (45 and 44 aa) straddling a middle, flexible segment (130 aa) [11]. In order to get information whether the structural and functional properties of TPPP/p25 are altered by the removal of the terminal segments, N- or C-terminal truncated versions of TPPP/p25 as well as double truncated TPPP/p25 form were produced by recombinant technique (Fig. 1).

The structural characteristics of these human recombinant TPPP/p25 forms were established by CD, FT-IR, fluorescence spectroscopy and limited proteolysis. As shown in Fig. 2A, the full length TPPP/p25 displayed a CD spectrum with a definitive minimum at 205 nm, characteristic for disordered proteins. Absence of either the N- or the C-terminus caused slight spectral alteration which became more pronounced in the case of the double truncated TPPP/p25: the position of the minimum shifted to a higher wavelength and the ratio of ellipticities measured at 222 nm and at the minimum increased (Fig. 2A).

To study whether this change can be attributed to the appearance of the β-sheet structure, FT-IR spectroscopy was carried out in the 1750-1500 cm^{-1} region which provides information on the Amide I-II bands [26-27]. We found that the FT-IR spectrum of the double truncated TPPP/p25 was not changed significantly as

compared to that of the full length protein (Fig. 2B). The main band of the Amide I region was at 1645 cm^{-1}, which mainly corresponds to random conformation, however, alpha-helix (typically around 1650-1660 cm^{-1}) and/or turns (1656-1671 cm^{-1}) structures could be involved. The slight shoulder at 1620 cm^{-1} present in the spectrum of the full length TPPP/p25 may indicate the occurrence of a not significant β-sheet structure which is not visible in the case of the double truncated form. In addition, minimal difference could be detected in the Amide II band (around 1565 cm^{-1}).

In a recent work we have established the presence of "molten globule" in the flexible middle segment of TPPP/p25 by fluorescence spectroscopy [28]. ANS fluorescence probe is appropriate to detect hydrophobic regions of proteins specifically if it is related to a molten globule state and not to globular or unfolded states [29-30]. As shown in Fig. 2C, the truncation of the unstructured tails of TPPP/p25 resulted in much less fluorescence intensity coupled with a smaller blue shift of the maximum of the emission spectrum. This finding could be indicative for the truncation-induced conformational change in the case of TPPP/p25.

Finally, a limited proteolysis study was performed with the full length and the double truncated TPPP/p25 forms since it is a sensitive tool to detect alteration in the structural integrity of proteins. The protein forms were digested with chymotrypsin, and the digests were analysed by SDS-PAGE. Fig. 2D illustrates the results of the time-dependent proteolysis: the full length protein was fully degraded after 40 minutes, while the double truncated TPPP/p25 displayed significantly less vulnerability towards the protease, even after 40 minutes two stable bands could be detected indicating the resistance of these two distinct partially digested forms against degradation. These data show that the truncation of both termini resulted in significant

structural alteration of the middle flexible segment, apparently it became more compact. Further investigations are needed for the identification of these stable structures.

3.2 Interaction of tubulin with the distinct TPPP/p25 forms

In order to determine whether the truncation-mediated changes in the structure of TPPP/p25 affect its physiologically relevant function, namely its interaction with tubulin, we investigated the tubulin binding, microtubule assembly promoting and microtubule bundling activities of the different TPPP/p25 forms.

The tubulin binding potency of the TPPP/p25 forms was analyzed by CD spectroscopy as we previously demonstrated by far-UV CD that the association of TPPP/p25 with tubulin produced a characteristic difference spectrum due to the structural alterations within the heterologous complex (Fig. 3A) [13]. A similar set of experiments with the truncated forms showed that the lack of N- and/or C-terminus reduced this effect to different extents; the double truncation virtually diminished the formation of the difference spectrum (Fig. A.1 and Fig. 3A). Thus it could be concluded that the disordered termini are directly or indirectly involved in the hetero-complex formation accompanied by CD spectral alteration.

The functional consequences of the truncation of TPPP/p25 on its tubulin polymerization promoting activity were investigated by turbidity measurements. Typical time courses of turbidity induced by the different TPPP/p25 forms revealed the distinct polymerization potency of the truncated forms as compared to the full length one (Fig. 3B). It can be unambiguously concluded that the double truncated form could not produce tubulin polymers with length larger than 350 nm causing turbidity. The tubulin polymerization potency of the N-terminal truncated and much more that of the C-terminal truncated form was reduced. These results demonstrate

that the disordered termini, even if in different extent, are involved in the tubulin polymerization activity of TPPP/p25.

Previously we reported that the TPPP/p25-induced tubulin polymerization promoting activity is coupled with the extensive bundling of the microtubules [13]. To test the bundling potency of the truncated forms, two sets of experiments were performed.

In one set of experiments the effects of the full length and truncated TPPP/p25 forms on the turbidity of paclitaxel-stabilized tubulin were tested. Fig. 3C shows that both the single and the double truncation of TPPP/p25 diminished its microtubule bundling activity suggesting that the disordered termini play significant role in the cross-linking of microtubules.

In a second set of experiments, a pelleting experiment was performed in which the partition of the TPPP/p25 between the pellet (microtubules) and the supernatant (tubulin) fraction was investigated.

As shown in Fig. 3D, both the TPPP/p25 forms and the tubulin were partitioned between the pellet and the supernatant fractions. While in the case of the full length TPPP/p25, the proteins were nearly equally partitioned between the pellet and the supernatant fractions, the amounts of both the tubulin and the truncated TPPP/p25 forms were reduced in the pellet fraction indicating the decreased polymerization potency of the truncated TPPP/p25 forms in accordance with the turbidity data (Fig. 3B). The reduced polymerization potency due to the truncation was the most pronounced for the double truncated TPPP/p25.

3.3 Intracellular localization of the TPPP/p25 forms in HeLa cell

As we revealed earlier TPPP/p25 co-localizes with the microtubule network in different cell lines expressing TPPP/p25 either exogenously (HeLa, CHO) or endogenously (CG-4), and the protein regulates the dynamics and organization of the

microtubule network via its microtubule bundling activity which enhances microtubule stability [16-17]. In order to obtain in vivo data for the role of the disordered terminal tails of TPPP/p25 in its microtubule-related function, HeLa cells were transiently transfected with the full length or the double truncated EGFP-TPPP/p25 and the intracellular localizations of the proteins were visualized by confocal microscopy after immunostaining for α-tubulin. Fig. 4 shows that while the full length TPPP/p25 tightly co-localized with the microtubule network in agreement with our earlier observations [16], the double truncated form distributed homogeneously within the cytoplasm. The finding that the double truncated TPPP/p25 cannot associate with the microtubule network underlines the role of the unstructured termini in the physiological function of TPPP/p25.

3.4 Interaction of α-synuclein with the distinct TPPP/p25 forms

It has been revealed that TPPP/p25 interacts with α-synuclein [22], and it is a potential inducer of α-synuclein fibrillation [23]. In order to identify the role of the disordered termini of TPPP/p25 in its pathological interaction, the binding of the TPPP/p25 forms to α-synuclein and their α-synuclein aggregation promoting activity were investigated first in vitro.

In an ELISA assay the affinities of the double truncated and the full length TPPP/p25 forms to α-synuclein were determined. The TPPP/p25 forms were immobilized on ELISA plates, then α-synuclein was added at different concentrations. Complex formation was detected by a specific α-synuclein antibody. α-synuclein bound to both TPPP/p25 forms (Fig. 5A) revealing that the binding motif is localized within the middle segment as suggested by our previous Pepscan experiment [22]. The binding affinities of the full length and the double truncated TPPP/p25 forms to α-synuclein

evaluated by curve fitting assuming simple hyperbolic saturation were found to be 0.59 ± 0.07 and 0.81 ± 0.09 μM, respectively.

Thioflavin T fluorescence measurement is a suitable method to follow the formation of amyloid-type (β-sheet rich) aggregates of α-synuclein [31] which likely occurs in the course of pathological inclusion formation as demonstrated earlier [23]. Fig. 5B shows that both the full length and the double truncated TPPP/p25 displayed similar α-synuclein aggregation promoting potency, while auto-aggregation of α-synuclein or the TPPP/p25 forms was not detected. The finding that the double truncated TPPP/p25 induced α-synuclein aggregation in concert with the ELISA data corroborates that the disordered terminal tails of TPPP/p25 are probably not involved in the formation of the pathological heterocomplex.

3.5 Colocalization of TPPP/p25 forms with α-synuclein in CHO10 cells

In order to test the role of the unstructured termini in the α-synuclein aggregation promoting activity of TPPP/p25, an in vivo cell model was established.

A CHO10 cell line that expresses full length TPPP/p25 ectopically following doxycyclin induction [17] was established as an appropriate system since these cells could take up α-synuclein from the culture media (Fig. 6A). This finding is in agreement with a recent report that demonstrates the transcellular spread of secreted α-synuclein oligomers in human H4 neuroglioma cells by exosomal transmission [32]. Here we show that TPPP/p25 can also be taken up by both the CHO10 and the HeLa cell lines as demonstrated by Western-blot (Fig. A.2) and the cellular uptake of both the full length and the double truncated TPPP/p25 can be visualized by fluorescence microscopy (Fig. 6B and 6C) just as that of α-synuclein (Fig. 6A). The intracellular appearance of α-synuclein or the double truncated TPPP/p25, but not the full length TPPP/p25 resulted in the formation of aggregates in a few cases (Fig. 6A and C vs B).

The α-synuclein aggregation promoting activity of the TPPP/p25 forms was characterized in CHO10 cells with and without the expression of the full length TPPP/p25. As shown in Fig. 7, co-aggregation of α-synuclein with either the full length or the double truncated TPPP/p25 forms can be visualized in non-induced CHO10 cells where all these proteins were taken up by the cells from the medium after their premixing (Fig. 7 lane 3 and 4, respectively). The added double truncated TPPP/p25 apparently displayed higher aggregation promoting activity as compared to the full length one, probably due to the fact that it is unable to bind to the microtubule network (cf. Fig. 4) therefore its free intracellular level is higher resulting in more pronounced α-synuclein aggregation promoting activity. The expression of the full length TPPP/p25 after doxycyclin induction only slightly contributed to α-synuclein aggregate formation (Fig. 7, lane 1 vs lane 3). The expressed full length TPPP/p25 rather co-localized with the microtubule network than with α-synuclein (Fig. 7 lane 1 and 2, Fig. A.3) as its binding affinity to tubulin is higher than to α-synuclein [22]. In contrast, when double truncated TPPP/p25 was added to the medium in addition to the TPPP/p25 expression, the aggregates increased in number and size (Fig. 7 lane 2 vs lane 1), which confirms the more pronounced α-synuclein aggregation promoting potency of the double truncated TPPP/p25 and strengthens our suggestion that it is because of its higher free intracellular level due to its inability to bind to microtubules. Nevertheless, these findings provide evidence for the intracellular association of both TPPP/p25 forms with α-synuclein and support that the disordered termini do not take part in the formation of pathological aggregates.

The extracellular transmission of these disordered hallmark proteins seems to have pathological significance and may explain how the co-enrichment of α-synuclein and TPPP/p25 could be evolved in the case of PD and Multiple System Atrophy in

neurons and oligodendroglia cells, respectively, though under physiological conditions these cells do not express these two proteins simultaneously. Indeed, the presence of both α-synuclein and TPPP/p25 was detected in the cerebrospinal fluid of human patients previously [19, 33-34].

3.6 Validation of the tubulin and α-synuclein binding motives of TPPP/p25

To validate the binding motives within the C-terminus (44 aa) and the middle flexible segment (130 aa) of TPPP/p25 that are predominantly involved in its heteroassociation with tubulin and α-synuclein, respectively, special ELISA experiments were performed with synthesized TPPP/p25 peptides.

For the identification of the tubulin binding motif of TPPP/p25, peptides were designed and synthesized according to data obtained with the truncated forms as compared to the full length TPPP/p25 and prediction based on the sequence homology between TPPP/p25 and the tubulin binding site of tau [35]:

tubulin binding motif of tau: ^{315}VYKPVDLSKVTSKCGSLGNIHHKPGGGQ^{341};

C-terminal tail of TPPP/p25: ^{163}VSRLTDTTKFT - - - GSHKERFDPSGKGK^{187}.

Accordingly, the following overlapping decapeptides were synthesized with a Cys residue that rendered possible their direct immobilization to an ELISA plate via their SH groups:

P1 C^{163}VSRLTDTTKF^{172}

P2 C^{168}DTTKFTGSHK^{177}

P3 C^{173}TGSHKERFDP^{182}

P4 C^{178}ERFDPSGKGK^{187}

Tubulin at different concentrations was added to the immobilized peptides; the peptide-bound tubulin was quantified with a tubulin antibody as described in the Materials and Methods.

The P4 peptide (178-187 aa) bound to tubulin with comparable affinity as TPPP/p25 (Kd = 0.135 ± 0.041 and 0.180 ± 0.030 μM for TPPP/p25 and P4 peptide, respectively), while the three other peptides displayed lower affinity (Fig. 8). Accordingly, the ^{178}ERFDPSGKGK^{187} segment of the C-terminal tail is the key binding motif on TPPP/p25 responsible for tubulin binding. Nevertheless, this issue does not exclude the involvement of other parts such as the N-terminal tail in the function of TPPP/p25 as noticed in the case of the turbidity measurements (cf. Fig. 3).

To reinforce the localization of the α-synuclein binding motif in a specific segment of the middle region of TPPP/p25 suggested by the Pepscan data, ^{147}KAPIISGVTKAISSPTVSRL^{166} [22], ELISA experiments were performed with biotinylated decapeptides. The peptides were synthetized to cover the potential α-synuclein binding segment. The decapeptides with biotinylated tag rendered it possible to test the binding potency of the α-synuclein directly to the peptides immobilized on a streptavidin-covered plate. To test whether the biotinylation of the peptides at one of their termini affects the interactions, modification of one of the peptides at N- or C-terminus was alternatively performed as shown below:

BF180: C-biotinylated: Ac-^{142}RLIEGKAPII^{151}K-NH_2

BF181: N-biotinylated: H-^{142}RLIEGKAPII^{151} -NH_2

BF182: C-biotinylated: Ac-^{147}KAPIISGVTK^{156}-NH_2

BF183: C-biotinylated: Ac-^{157}AISSPTVSRL^{166}K -NH_2

There is no significant difference in the binding affinity of the α-synuclein to the immobilized peptides as revealed by a specific α-synuclein antibody (Fig. 9A). The apparent affinity constants (Kd) obtained by fitting the experimental points with a simple hyperbolic saturation curve were 2.91 ± 0.69, 3.60 ± 0.57, 4.15 ± 0.24 and 4.01 ± 0.18 μM for the BF180, BF181, BF182 and BF183 peptides, respectively;

which are significantly higher than that determined for the double truncated (0.81 ± 0.09 μM) and for the full length (0.59 ± 0.07 μM) TPPP/p25 (cf. Fig. 5A). The α-synuclein binding is apparently independent of the nature of the decapeptides selected as well as the position of the biotinylation label. Consequently one can conclude that the binding is independent of the position of the biotinylation, but cannot exclude its role in the binding.

Another, competitive ELISA experiment was carried out with the biotinylated peptides, however, they were premixed with α-synuclein in solution then added to the full length or double truncated TPPP/p25 forms immobilized on ELISA plates. The inhibitory effect of the peptides on the binding of α-synuclein to TPPP/p25 forms was detected by a specific α-synuclein antibody. In the experiment presented in Fig. 9B, α-synuclein was added at constant concentration which corresponded roughly to the half saturation value (cf. Fig. 5A), and the peptides were preincubated with α-synuclein at 10 and 20 μM concentrations. The results showed that i) there was a single peptide, BF182, which inhibited the heteroassociation of the α-synuclein with TPPP/p25; ii) the extent of the inhibition was similar in the case of the full length and the double truncated protein; iii) the inhibitory effect of the BF182 was concentration-dependent; iv) the BF180, BF181 and BF183 peptides were virtually ineffective concerning their inhibitory effects on the heteroassociation independently of the position of the biotinylation. These data seem to contradict the direct binding data where the α-synuclein displayed similar affinity to each biotinylated TPPP/p25 peptide (Kd ~ 4 μM), in addition, this affinity was lower as determined for the full length/double truncated protein (Kd = 0.59 μM / 0.81 μM). A plausible way to interpret these ELISA data is that the disordered α-synuclein may have another

binding segment interacting with the biotinylated TPPP/p25 peptides, but the segment is out of the contact surface of the TPPP/p25-α-synuclein pathological complex.

The findings with the peptides and truncated TPPP/p25 forms suggest that the amino acids and/or short peptides within the middle segment of TPPP/p25 could generate a specific structure such as a foldamer, for the α-synuclein binding to form the pathologically relevant heteroassociation leading to aggregation.

4. CONCLUSIONS

In conclusion, TPPP/p25 is a protein with a neomorphic moonlighting feature that is related to its disordered structure which permits multiple interactions with distinct proteins forming physiological or pathological complexes. In this paper the structural and functional features of the disordered N- and C-terminal tails of TPPP/p25 were characterized. Our data revealed the key role of the C-terminus and the fact that the N-terminus is also involved, even if to a much less extent, in its physiological function related to the modulation of the dynamics and organization of the microtubule network. In contrast, the α-synuclein binding and aggregation promoting activity of TPPP/p25 is virtually not influenced by the truncation of the terminal tails.

Experiments with designed and synthesized TPPP/p25 peptides rendered it possible to validate the binding motives for tubulin and α-synuclein (Fig. 10). The ELISA experiments with decapeptides covering the potential tubulin and α-synuclein binding segments localized these binding motives on the C-terminal tail (^{178}ERFDPSGKGK^{187}) and within the middle region (^{147}KAPIISGVTK^{156}) of TPPP/p25, respectively. The results obtained with the overlapping decapeptides may allow one to further reduce the binding motives to five-amino-acid segments which are substantial for the formation and maintenance of physiological and pathological heterocomplexes. The distinct localization of these binding motives in the disordered

TPPP/p25 assigns its neomorphic moonlighting functions and has innovative potential in the development of anti-synucleinopathy drugs.

5. LIST OF ABBREVIATIONS USED

1-anilino naphthalene-8-sulfonic acid, ANS; bovine serum albumin, BSA; circular dichroism, CD; 4,6-diamidino-2-phenylindole, DAPI; dithioerythritol, DTE; enzyme-linked immunosorbent assay, ELISA; Fourier transformed infrared spectroscopy, FT-IR; glyceraldehyde 3-phosphate dehydrogenase, GAPDH; Parkinson's disease, PD; phosphate buffered saline, PBS; polymerase chain reaction, PCR; sodium dodecyl sulfate polyacrylamide gel electrophoresis, SDS-PAGE; solid phase peptide synthesis, SPPS; Tubulin Polymerization Promoting Protein, TPPP/p25.

6. COMPETING INTERESTS

The authors declare no conflict of interest.

7. ACKNOWLEDGEMENTS

This work was supported by the European Commission [(DCI ALA/19.09.01/10/21526/ 245-297/ALFA 111(2010)29], European Concerted Research Action [COST Action TD0905]; Hungarian National Scientific Research Fund Grants OTKA T-101039 and Richter Gedeon Nyrt (4700147899) to J. Ovádi. The funding body had no role in design, collection, analysis and interpretation of data, or in the writing of the manuscript.

8. REFERENCES

[1] G. Wistow, J. Piatigorsky, Recruitment of enzymes as lens structural proteins, Science 236 (1987) 1554-1556.

[2] J. Piatigorsky, G.J. Wistow, Enzyme/crystallins: gene sharing as an evolutionary strategy, Cell 57 (1989) 197-199.

[3] C.J. Jeffery, Moonlighting proteins, Trends Biochem. Sci. 24 (1999) 8-11.

[4] C.J. Jeffery, Proteins with neomorphic moonlighting functions in disease, IUBMB Life 63 (2011) 489-494.

[5] J. Oláh, N. Tőkési, A. Lehotzky, F. Orosz, J. Ovádi, Moonlighting microtubule-associated proteins: Regulatory functions by day and pathological functions at night, Cytoskeleton (Hoboken). (2013) doi: 10.1002/cm.21137. [Epub ahead of print]

[6] A.L. Fink, Natively unfolded proteins, Curr. Opin. Struct. Biol. 15 (2005) 35-41.

[7] P. Tompa, C. Szász, L. Buday, Structural disorder throws new light on moonlighting, Trends Biochem Sci. 30 (2005) 484-489.

[8] A.K. Dunker, I. Silman, V.N. Uversky, J.L. Sussman, Function and structure of inherently disordered proteins, Curr. Opin. Struct. Biol. 18 (2008) 756-764.

[9] V.N. Uversky, What does it mean to be natively unfolded?, Eur. J. Biochem. 269 (2002) 2–12.

[10] G.B. Irvine, O.M. El-Agnaf, G.M. Shankar, D.M. Walsh, Protein aggregation in the brain: the molecular basis for Alzheimer's and Parkinson's diseases, Mol. Med. 14 (2008) 451-464.

[11] A. Zotter, A. Bodor, J. Oláh, E. Hlavanda, F. Orosz, A. Perczel, J. Ovádi, Disordered TPPP/p25 binds GTP and displays Mg(2+)-dependent GTPase activity, FEBS Lett. 585 (2011) 803-808.

[12] M. Takahashi, K. Tomizawa, K. Ishiguro, K. Sato, A. Omori, S. Sato, A. Shiratsuchi, T. Uchida, K. Imahori, A novel brain-specific 25 kDa protein (p25) is phosphorylated by a Ser/Thr-Pro kinase (TPK II) from tau protein kinase fractions, FEBS Lett. 289 (1991) 37-43.

[13] E. Hlavanda, J. Kovács, J. Oláh, F. Orosz, K.F. Medzihradszky, J. Ovádi, Brain-specific p25 protein binds to tubulin and microtubules and induces aberrant microtubule assemblies at substoichiometric concentrations, Biochemistry 41 (2002) 8657-8664.

[14] M. Takahashi, K. Tomizawa, S.C. Fujita, K. Sato, T. Uchida, K. Imahori, A brain-specific protein p25 is localized and associated with oligodendrocytes, neuropil, and fiber-like structures of the CA hippocampal region in the rat brain, J. Neurochem. 60 (1993) 228-235.

[15] A. Lehotzky, P. Lau, N. Tőkési, N. Muja, L.D. Hudson, J. Ovádi, Tubulin polymerization-promoting protein (TPPP/p25) is critical for oligodendrocyte differentiation, Glia 58 (2010) 157-168.

[16] A. Lehotzky, L. Tirián, N. Tőkési, P. Lénárt, B. Szabó, J. Kovács, J. Ovádi, Dynamic targeting of microtubules by TPPP/p25 affects cell survival, J. Cell. Sci. 117 (2004) 6249-6259.

[17] N. Tőkési, A. Lehotzky, I. Horváth, B. Szabó, J. Oláh, P. Lau, J. Ovádi, TPPP/p25 promotes tubulin acetylation by inhibiting histone deacetylase 6, J. Biol. Chem. 285 (2010) 17896-17906.

[18] R. Höftberger, S. Fink, F. Aboul-Enein, G. Botond, J. Oláh, T. Berki, J. Ovádi, H. Lassmann, H. Budka, G.G. Kovacs, Tubulin polymerization promoting protein (TPPP/p25) as a marker for oligodendroglial changes in multiple sclerosis, Glia 58 (2010) 1847-1857.

[19] O. Vincze, J. Oláh, D. Zádori, P. Klivényi, L. Vécsei, J. Ovádi, A new myelin protein, TPPP/p25, reduced in demyelinated lesions is enriched in cerebrospinal fluid of multiple sclerosis, Biochem. Biophys. Res. Commun. 409 (2011) 137-141.

[20] M. Preusser, A. Lehotzky, H. Budka, J. Ovádi, G.G. Kovacs, TPPP/p25 in brain tumours: expression in non-neoplastic oligodendrocytes but not in oligodendroglioma cells, Acta Neuropathol. 113 (2007) 213-215.

[21] G.G. Kovacs, L. László, J. Kovács, P.H. Jensen, E. Lindersson, G. Botond, T. Molnár, A. Perczel, F. Hudecz, G. Mező, A. Erdei, L. Tirián, A. Lehotzky, E. Gelpi, H. Budka, J. Ovádi, Natively unfolded tubulin polymerization promoting protein TPPP/p25 is a common marker of alpha-synucleinopathies, Neurobiol. Dis. 17 (2004) 155-162.

[22] J. Oláh, O. Vincze, D. Virok, D. Simon, Z. Bozsó, N. Tőkési, I. Horváth, E. Hlavanda, J. Kovács, A. Magyar, M. Szűcs, F. Orosz, B. Penke, J. Ovádi, Interactions of pathological hallmark proteins: tubulin polymerization promoting protein/p25, beta-amyloid, and alpha-synuclein, J. Biol. Chem. 286 (2011) 34088-34100.

[23] E. Lindersson, D. Lundvig, C. Petersen, P. Madsen, J.R. Nyengaard, P. Hojrup, T. Moos, D. Otzen, W.P. Gai, P.C. Blumbergs, P.H. Jensen, p25alpha Stimulates alpha-synuclein aggregation and is co-localized with aggregated alpha-synuclein in alpha-synucleinopathies, J. Biol. Chem. 280 (2005) 5703-5715.

[24] C.N. Na, S.N. Timasheff, Interaction of vinblastine with calf brain tubulin: multiple equilibria, Biochemistry 25 (1986) 6214-6222.

[25] S.R. Paik, J.H. Lee, D.H. Kim, C.S. Chang, J. Kim, Aluminum-induced structural alterations of the precursor of the non-A beta component of Alzheimer's disease amyloid, Arch. Biochem. Biophys. 344 (1997) 325-334.

[26] W.K. Surewicz, H.H. Mantsch, D. Chapman, Determination of protein secondary structure by Fourier transform infrared spectroscopy: a critical assessment, Biochemistry 32 (1993) 389-394.

[27] M. Pivato, G. De Franceschi, L. Tosatto, E. Frare, D. Kumar, D. Aioanei, M. Brucale, I. Tessari, M. Bisaglia, B. Samori, P.P. de Laureto, L. Bubacco, Covalent α-synuclein dimers: chemico-physical and aggregation properties, PLoS One 7 (2012) e50027.

[28] Á. Zotter, J. Oláh, E. Hlavanda, A. Bodor, A. Perczel, K. Szigeti, J. Fidy, J. Ovádi, Zn^{2}+-induced rearrangement of the disordered TPPP/p25 affects its microtubule assembly and GTPase activity, Biochemistry 50 (2011) 9568-9578.

[29] G.V. Semisotnov, N.A. Rodionova, O.I. Razgulyaev, V.N. Uversky, A.F. Gripas, R.I. Gilmanshin, Study of the "molten globule" intermediate state in protein folding by a hydrophobic fluorescent probe, Biopolymers 31 (1991) 119-128.

[30] S.S. Leal, C.M. Gomes, Studies of the molten globule state of ferredoxin: structural characterization and implications on protein folding and iron-sulfur center assembly, Proteins 68 (2007) 606-616.

[31] A. Hawe, M. Sutter, W. Jiskoot, Extrinsic fluorescent dyes as tools for protein characterization, Pharm. Res. 25 (2008) 1487-1499.

[32] K.M. Danzer, L.R. Kranich, W.P. Ruf, O. Cagsal-Getkin, A.R. Winslow, L. Zhu, C.R. Vanderburg, P.J. McLean, Exosomal cell-to-cell transmission of alpha synuclein oligomers, Mol. Neurodegener. 7 (2012) 42.

[33] R. Borghi, R. Marchese, A. Negro, L. Marinelli, G. Forloni, D. Zaccheo, G. Abbruzzese, M. Tabaton, Full length alpha-synuclein is present in

cerebrospinal fluid from Parkinson's disease and normal subjects, Neurosci. Lett. 287 (2000) 65-67.

[34] O. Marques, T.F. Outeiro, Alpha-synuclein: from secretion to dysfunction and death, Cell Death Dis. 3 (2012) e350.

[35] E. Hlavanda, E. Klement, E. Kokai, J. Kovács, O. Vincze, N. Tőkési, F. Orosz, K.F. Medzihradszky, V. Dombrádi, J. Ovádi, Phosphorylation blocks the activity of tubulin polymerization-promoting protein (TPPP): identification of sites targeted by different kinases, J. Biol. Chem. 282 (2007) 29531-29539.

9. FIGURE LEGENDS

Figure 1 - Scheme of the different TPPP/p25 forms (A) with the SDS/PAGE images (B).

(B) MM: molecular weight marker, lane 1: TPPP/p25, lane 2: N-terminal truncated TPPP/p25, lane 3: C-terminal truncated TPPP/p25, lane 4: double truncated TPPP/p25.

Figure 2 - Structural characterization of the different TPPP/p25 forms.

(A) Normalized far-UV CD spectra. TPPP/p25 (bold line), N-terminal truncated TPPP/p25 (solid line), C-terminal truncated TPPP/p25 (dashed line), double truncated TPPP/p25 (dotted line). The standard error of the determinations (SEM) was ± 10% (n=3). (B) FT-IR spectrum of the full length (bold line) and the double truncated (dotted line) TPPP/p25. (C) ANS fluorescence spectroscopy. Emission spectra of free ANS (dash-dot-dotted line), ANS with full length (bold line) and double truncated (dotted line) TPPP/p25. The concentration of protein and ANS was 50 μM and 2.5 μM, respectively. The standard error of the determinations (SEM) was ± 10% (n=3-5). (D) Time-dependent limited proteolysis of the full length and the double truncated TPPP/p25 with chymotrypsin terminated at 0, 10, 20 and 40 minutes and analyzed by

SDS-PAGE. A representative experiment is presented. The standard error of the determinations (SEM) was ± 10% (n=3-4).

Figure 3 - Interaction of tubulin with the distinct TPPP/p25 forms.

(A) Difference CD spectra of TPPP/p25 forms and tubulin. Difference ellipticity was calculated by subtracting the ellipticities of tubulin and the TPPP/p25 forms from that measured with their mixtures. The concentration of tubulin was 1 μM, while that of the TPPP/p25 forms was 4 μM. (B) The tubulin polymerization promoting potency of the TPPP/p25 forms followed by turbidimetry. The polymerization of 7 μM tubulin to microtubules was induced by the addition of 3 μM of each TPPP/p25 form. (C) The microtubule bundling potency of the TPPP/p25 forms as determined by a turbidimetric assay. Tubulin (10 μM) polymerization was induced by paclitaxel (20 μM), and TPPP/p25 (3 μM) forms were added subsequently. (D) Pelleting experiment. 5 μM tubulin was incubated with 10 μM of each TPPP/p25 form in polymerization buffer. After centrifugation, the pellet/microtubule (P) and the supernatant/tubulin (S) fractions were separated and analysed by SDS-PAGE on a Tris-Tricine two-layer gel. TPPP/p25 (bold line), N-terminal truncated TPPP/p25 (solid line), C-terminal truncated TPPP/p25 (dashed line), double truncated TPPP/p25 (dotted line) (A-C). The standard error of the determinations (SEM) was ± 10% (n=3-5).

Figure 4 - Localization of the TPPP/p25 forms in HeLa cells.

Transiently transfected cells with pEGFP-TPPP/p25 (A-C, green) or pEGFP-double truncated TPPP/p25 (D-F, green) were immunostained with α-tubulin antibody (red) and visualized by confocal microscopy. Note the co-localization of TPPP/p25 along the microtubule network (C) in contrast to the homogenous distribution of the double truncated TPPP/p25 within the cytoplasm (F). Nuclei were counterstained with DAPI

(blue). Scale bar: 10 μm.

Figure 5 - The interaction of the full length and the double truncated TPPP/p25 forms with α-synuclein.

(A) ELISA experiment. The plate was coated with TPPP/p25 (●, ▲, ◆, ▼) or the double truncated form of the protein (○, △, ◇, ▽), then α-synuclein was added at different concentrations. The different symbols indicate independent experiments. The normalized ELISA data were calculated as the absorbance at a given α-synuclein concentration divided by the absorbance at saturation. The binding affinities of the full length (bold line) and the double truncated (dashed line) TPPP/p25 forms to α-synuclein were evaluated by curve fitting assuming simple hyperbolic saturation. (B) Aggregation of α-synuclein induced by the different TPPP/p25 forms followed by thioflavin T fluorescence emission at 480 nm. 150 μM α-synuclein was incubated in the absence and presence of 10 μM TPPP/p25 or double truncated TPPP/p25 in PBS buffer for 4 days at 37 °C, and the samples were analyzed by Thioflavin T fluorescence. TPPP/p25 or the double truncated TPPP/p25 alone was incubated under the same conditions. The spectrum of Thioflavin T was subtracted from that of the sample in each case. Error bars represent the standard error of the determinations (SEM) (n=3). * Significant difference between α-synuclein and α-synuclein incubated with the full length or the double truncated TPPP/p25 (according to the Student's t-test, $p<0.05$).

Figure 6 - Cellular uptake of α-synuclein or the TPPP/p25 forms as detected by immunofluorescence microscopy.

Non-induced CHO10 cells took up human recombinant α-synuclein (A, red) or the TPPP/p25 forms (B and C, red) from the cell culture media as visualized by immunostaining for α-synuclein or TPPP/p25, respectively. The TPPP/p25 forms

were stained by the same antibody [21]. Nuclei were counterstained with DAPI (blue). Scale bar: 2.5 μm.

Figure 7 - Intracellular localization of the TPPP/p25 forms and α-synuclein in CHO10 cells as detected by immunofluorescence microscopy.

CHO10 cells with (lane 1-2) and without (lane 3-4) full length TPPP/p25 expression took up full length (lane 1 and 3, red) or double truncated (lane 2 and 4, red) TPPP/p25 and α-synuclein (lane 1-4, green) from the medium after premixing as visualized by immunostaining for TPPP/p25 and α-synuclein, respectively. Note that either the expressed (lane 1 and 2) or the added full length TPPP/p25 (arrowhead at lane 3) was rather colocalized with the microtubule network than with α-synuclein. The double truncated TPPP/p25 and α-synuclein were co-enriched in cytoplasmic aggregates (lane 2 and 4) which were more pronounced both in number and size than the aggregates induced by full length TPPP/p25 expression (lane 1) or uptake (lane 3). Nuclei were counterstained with DAPI (blue). Scale bar: 2.5 μm.

Figure 8 - The interaction of TPPP/p25 and the decapeptides with tubulin followed by ELISA.

The plate was coated with the P1-P4 peptides or TPPP/p25 via their SH groups, then it was incubated with tubulin at different concentrations. TPPP/p25 (●), P1 (Δ), P2 (○), P3 (◊) and P4 (▲).

Figure 9 - The interaction of decapeptides with α-synuclein followed by ELISA and the effect of biotinylated peptides on TPPP/p25 – α-synuclein interaction.

(A) The plate was coated with streptavidin, then the biotinylated peptides were added to the plate. Next it was incubated with α-synuclein at different concentrations. BF180 (●, solid line), BF181 (○, dashed line), BF182 (▲, dotted line) and BF183 (Δ, dash-dot-dotted line). (B) The plate was coated with the full length (white column) or

the double truncated (black column) TPPP/p25 form. Then 500 nM α-synuclein preincubated with the biotinylated peptides BF180-183 (10 and 20 μM) was added to the plate. The interaction was detected by an α-synuclein antibody. Error bars represent the standard error of the determinations (SEM) (n=3).

Figure 10 - Scheme of the tubulin and α-synuclein binding motives of TPPP/p25 as validated by different TPPP/p25 peptides.

Localization of the different TPPP/p25 peptides in the sequence of TPPP/p25 and the amino acid sequence of the potential binding site of tubulin (green) and α-synuclein (blue) are shown in red frames.

Figure 1.

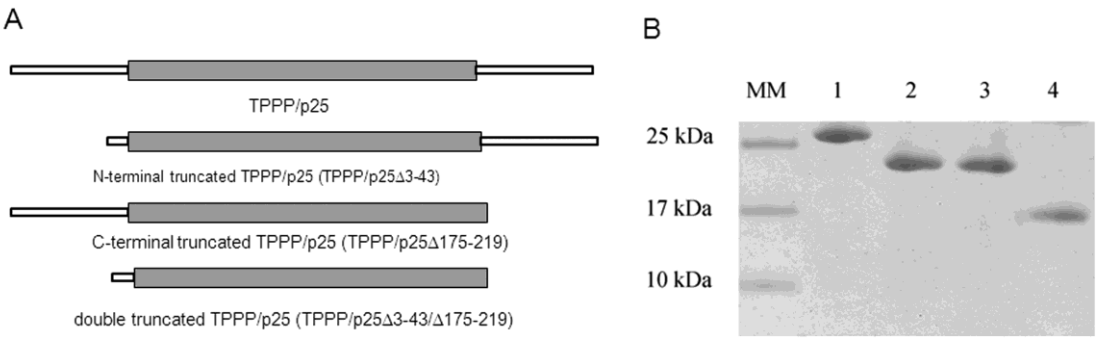
A
TPPP/p25
N-terminal truncated TPPP/p25 (TPPP/p25Δ3-43)
C-terminal truncated TPPP/p25 (TPPP/p25Δ175-219)
double truncated TPPP/p25 (TPPP/p25Δ3-43/Δ175-219)
B
MM
1
2
3
4
25 kDa
17 kDa
10 kDa

Figure 2.

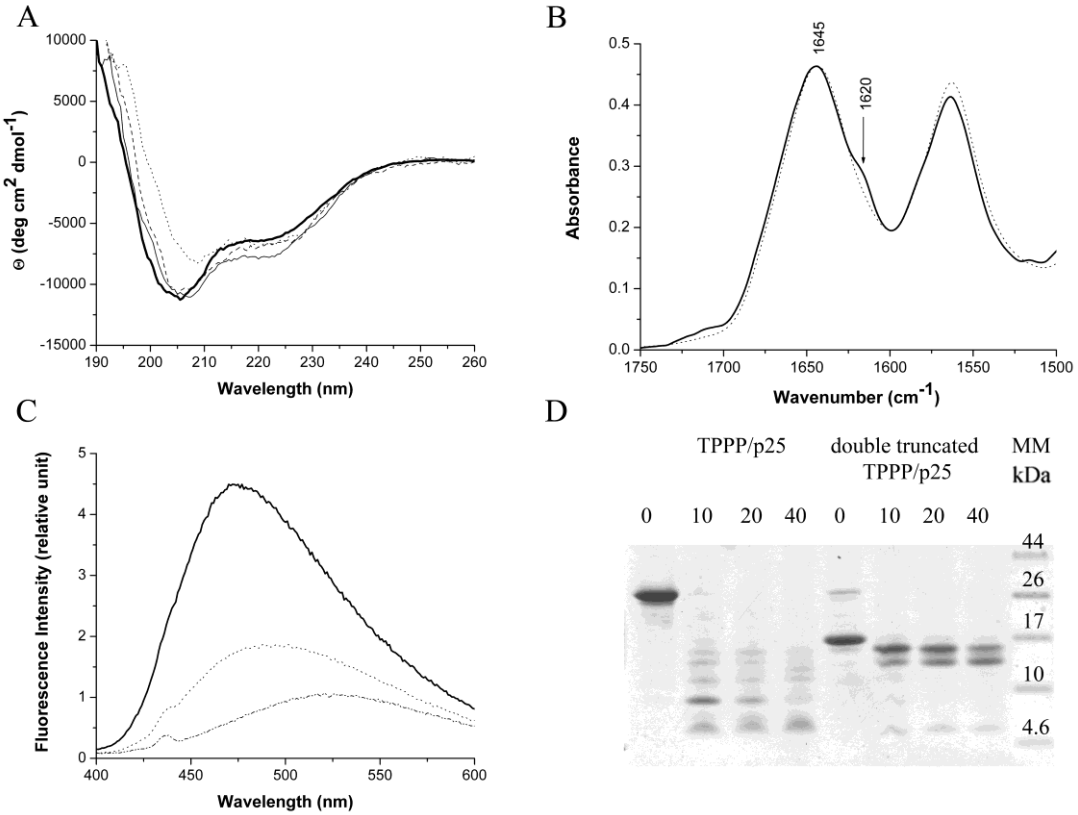
A
Θ (deg cm2 dmol-1)
Wavelength (nm)
B
Absorbance
1645
1620
Wavenumber (cm-1)
C
Fluorescence Intensity (relative unit)
Wavelength (nm)
D
TPPP/p25
double truncated TPPP/p25
MM kDa
0 10 20 40 0 10 20 40
44
26
17
10
4.6

Figure 3.

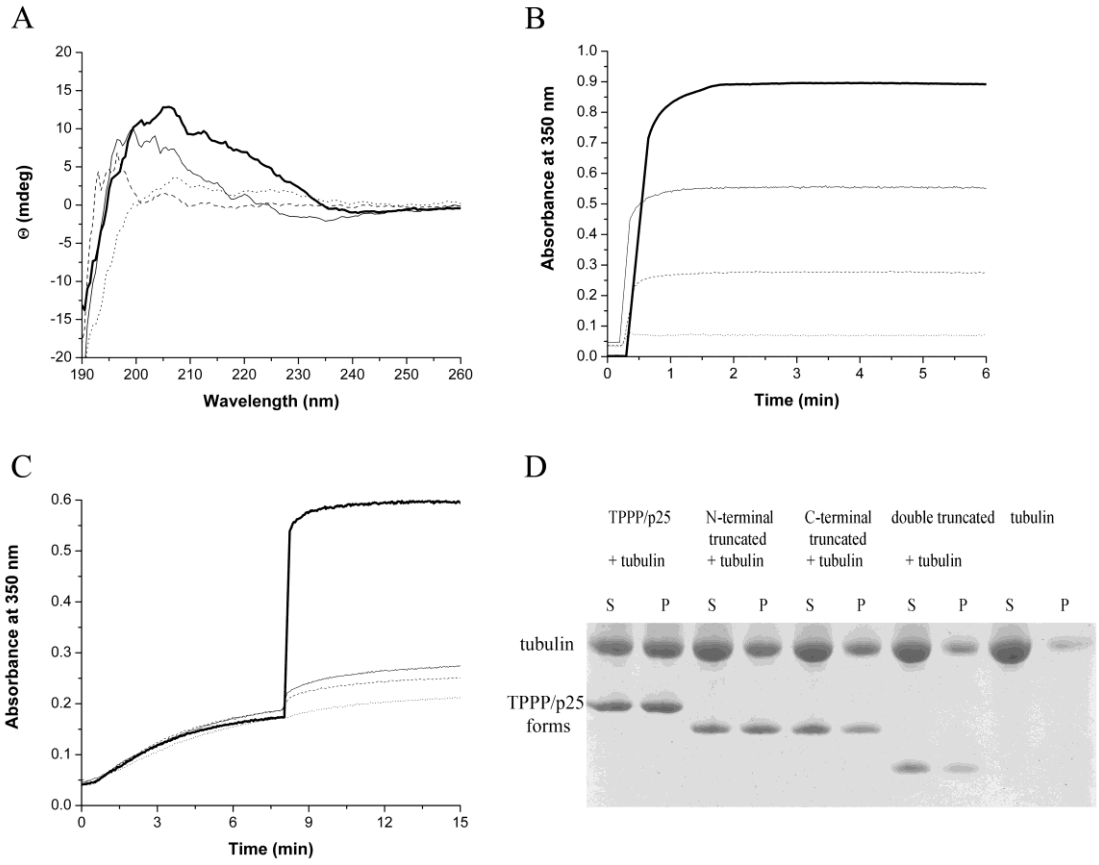
A
Θ (mdeg)
Wavelength (nm)
B
Absorbance at 350 nm
Time (min)
C
Absorbance at 350 nm
Time (min)
D
TPPP/p25 + tubulin
N-terminal truncated + tubulin
C-terminal truncated + tubulin
double truncated + tubulin
tubulin
S
P
tubulin
TPPP/p25 forms

Figure 4.

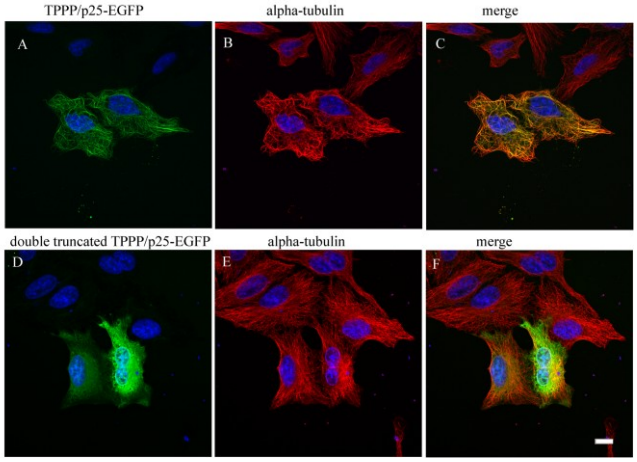
TPPP/p25-EGFP
alpha-tubulin
merge
A
B
C
double truncated TPPP/p25-EGFP
alpha-tubulin
merge
D
E
F

Figure 5.

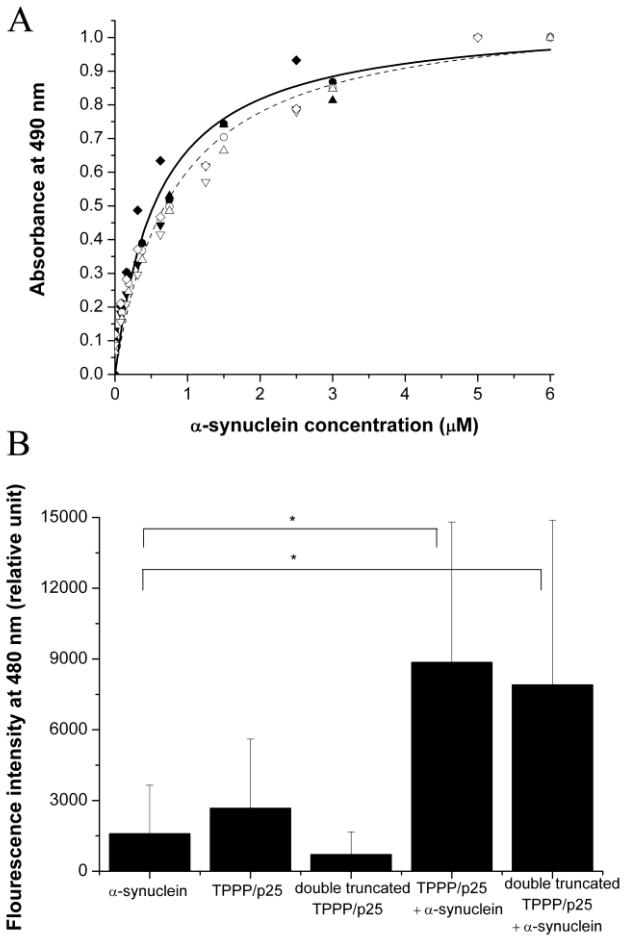
A
Absorbance at 490 nm
α-synuclein concentration (μM)
B
Flourescence intensity at 480 nm (relative unit)
α-synuclein
TPPP/p25
double truncated TPPP/p25
TPPP/p25 + α-synuclein
double truncated TPPP/p25 + α-synuclein

Figure 6.

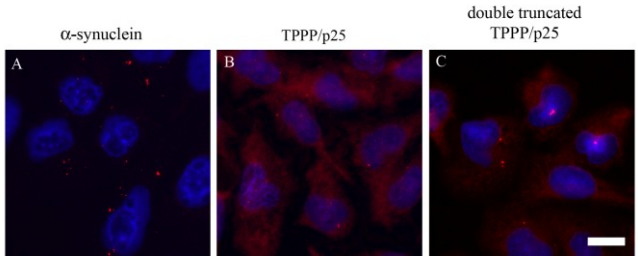

Figure 7.

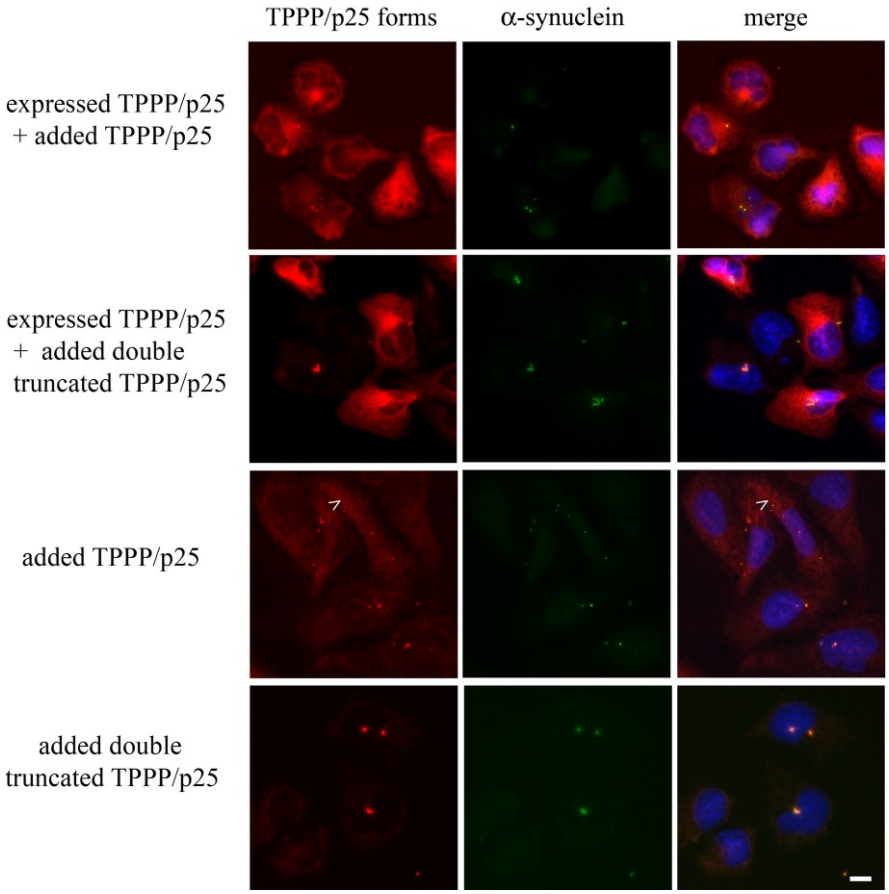
TPPP/p25 forms
α-synuclein
merge
expressed TPPP/p25 + added TPPP/p25
expressed TPPP/p25 + added double truncated TPPP/p25
added TPPP/p25
added double truncated TPPP/p25

Figure 8.

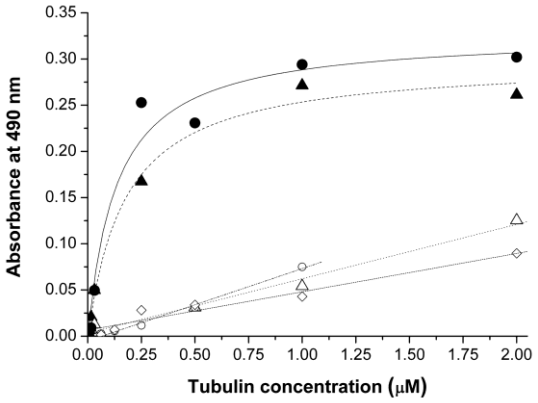
Absorbance at 490 nm
0.35
0.30
0.25
0.20
0.15
0.10
0.05
0.00
0.00
0.25
0.50
0.75
1.00
1.25
1.50
1.75
2.00
Tubulin concentration (μM)

Figure 9.

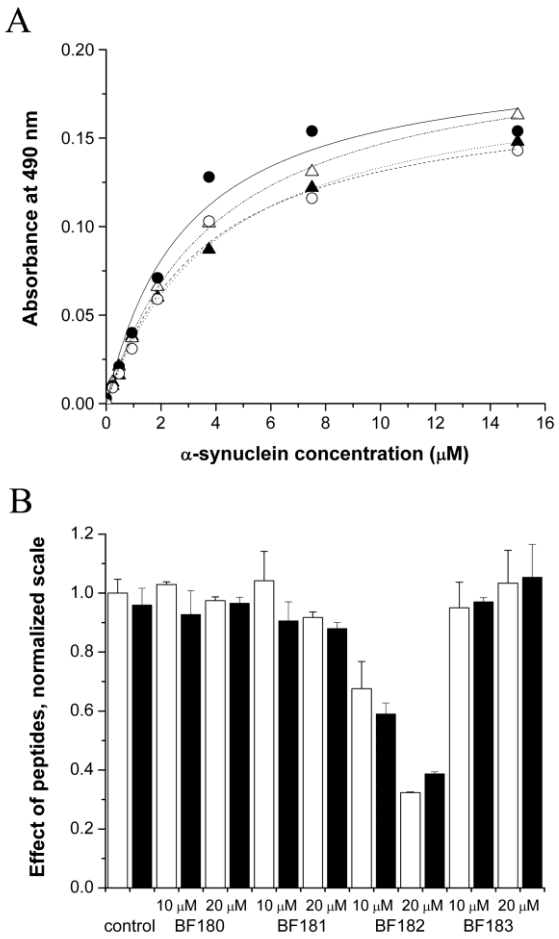
A
Absorbance at 490 nm
0.20
0.15
0.10
0.05
0.00
0
2
4
6
8
10
12
14
16
α-synuclein concentration (μM)
B
Effect of peptides, normalized scale
1.2
1.0
0.8
0.6
0.4
0.2
0.0
10 μM
20 μM
control
BF180
BF181
BF182
BF183

Figure 10.

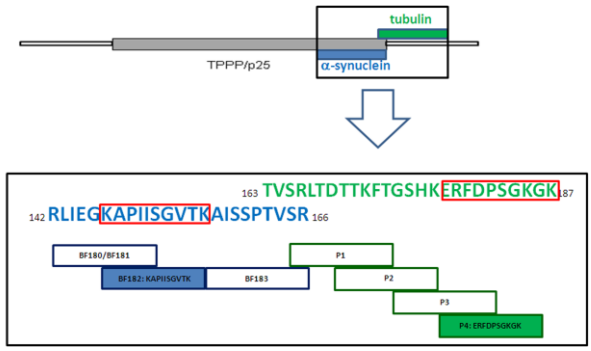
tubulin
TPPP/p25
α-synuclein
163 TVSRLTDTTKFTGSHKERFDPSGKGK 187
142 RLIEGKAPIISGVTKAISSPTVSR 166
BF180/BF181
BF182: KAPIISGVTK
BF183
P1
P2
P3
P4: ERFDPSGKGK